Plant Physiology and Biochemistry 229 (2025) 110494

Contents lists available at ScienceDirect

Plant Physiology and Biochemistry

journal homepage: www.elsevier.com/locate/plaphy

Multi-omics analysis reveals molecular and biochemical mechanisms underlying alkaline stress adaptation in *Solanum lycopersicum* L

Bhargava Krishna Ganasula [a], Claudia Chiodi [a], Silvia Celletti [b], Riccardo Fedeli [c], Saptarathi Deb [a], Giovanni Bertoldo [a,*], Maria Cristina Della Lucia [a], Massimo Cagnin [a], Luisella Roberta Celi [b], Piergiorgio Stevanato [a]

[a] Department of Agronomy, Food, Natural Resources, Animals and Environment, University of Padova, Legnaro, (PD), Italy
[b] Department of Agriculture, Forest and Food Sciences, University of Torino, Grugliasco, (TO), Italy
[c] Department of Life Sciences, University of Siena, Siena, Italy

ARTICLE INFO

Keywords:
Alkaline stress
Amino acids
Ionomics
Osmo-regulation
Stress response
Tomato
Transcriptomics

ABSTRACT

Alkaline stress poses a major constraint that limits tomato (*Solanum lycopersicum* L.) productivity worldwide by disrupting ion homeostasis and causing oxidative damage, yet the underlying genotype-dependent mechanisms remain incompletely understood. This study employed an integrative multi-omics approach combining transcriptomics, targeted RT-qPCR validation, biochemical assays, and ionomic profiling to investigate contrasting responses in two tomato genotypes, A10 (tolerant) and M56 (sensitive). Plants were hydroponically grown under control (pH 5.9) and alkaline stress conditions (pH 8.2 and 9.2, adjusted with NaOH) in a controlled environment. Principal component analysis of the RNA-Seq data confirmed distinct genotype-dependent clustering under stress. Comprehensive transcriptomic analyses revealed that A10 exhibited extensive transcriptional reprogramming, with over 500 differentially expressed genes and significant enrichment of MAPK-ethylene signalling and glutamate decarboxylase (*SlGAD1*, *SlGAD2*) pathways, with RT-qPCR validation supporting differential expression of key ion transporters (*HKT1;1*, *HKT1;2*, *SOS1*). In contrast, M56 displayed minimal transcriptional adjustments (<50 DEGs). Biochemical analyses confirmed genotype-specific osmoprotectant accumulation: A10 showed significant increases in proline (+37 %) and polyphenols (+96 %) at high pH, while M56 levels declined. Free amino acid profiling further revealed that A10 maintained elevated GABA and glutamate content under stress, supporting metabolic adjustments that sustain osmotic balance. Ionomic analysis demonstrated that A10 effectively restricted Na^+ accumulation (4 and 5-fold increase) compared to M56's higher influx (6.5 and 9-fold), while maintaining K^+ levels and a more favourable K^+/Na^+ ratio. These integrated results indicate that A10's superior tolerance involves coordinated transcriptional, metabolic, and ionic responses that mitigate osmotic and oxidative stress. This work identifies robust candidate pathways and genes for breeding alkaline-tolerant tomato cultivars to support sustainable production in high-pH soils.

1. Introduction

Plants are exposed to complex environmental conditions influenced by multiple abiotic stress factors (Van Zelm et al., 2020). Among these, alkaline stress, caused by high soil pH, is a major constraint that disrupts nutrient uptake, physiological functions, and crop yield. Globally, over 434 million hectares of land are affected by alkaline and sodic soils, while approximately 10 % of the Earth's surface, including nearly 30 % of arable land, suffers from salinity or alkalinity (Van Zelm et al., 2020; Rao et al., 2023). Such widespread soil alkalinity poses a significant threat to agricultural productivity and food security worldwide. Enhancing crop tolerance to alkaline soils aligns with United Nations Sustainable Development Goal 2 (Zero Hunger), which emphasizes the need for sustainable agricultural practices to end hunger and ensure reliable access to nutritious food (FAO, 2021) (The State of Food Security, 2021). Alkaline soils, dominated by sodium bicarbonate ($NaHCO_3$) and sodium carbonate (Na_2CO_3), cause a sharp rise in pH, which alters apoplastic pH, disrupts cellular homeostasis, and leads to ionic

This article is part of a special issue entitled: Salinity and Plants published in Plant Physiology and Biochemistry.

* Corresponding author.
E-mail address: giovanni.bertoldo@unipd.it (G. Bertoldo).

https://doi.org/10.1016/j.plaphy.2025.110494
Received 14 March 2025; Received in revised form 5 September 2025; Accepted 5 September 2025
Available online 6 September 2025
0981-9428/© 2025 The Authors. Published by Elsevier Masson SAS. This is an open access article under the CC BY license (http://creativecommons.org/licenses/by/4.0/).

imbalance, osmotic stress, and nutrient precipitation collectively impairing plant growth and making alkaline stress more harmful than salinity stress alone (Zhang et al., 2023; Fang et al., 2021).

Tomato (*Solanum lycopersicum* L.), one of the most widely cultivated vegetable crops, is highly sensitive to abiotic stresses, particularly salinity and alkalinity, which severely limit yield and quality (Tsai and Schmidt, 2021; FAO, 2024). Modern tomato cultivars have lost much of the natural stress tolerance present in wild relatives (Yan et al., 2021; Ali et al., 2021). Alkaline stress negatively impacts seed germination, root and shoot development, photosynthesis, and overall plant metabolism, often through reactive oxygen species (ROS) accumulation, which leads to oxidative damage of proteins, lipids, and nucleic acids (Ali et al., 2021; Guo et al., 2022).

To counteract such stresses, tomato plants activate a range of physiological and biochemical defences, including the synthesis of amino acids, antioxidants, and organic acids, to mitigate osmotic stress (Aung et al., 2022; Wang et al., 2020a). Specifically, to cope with alkaline stress, tomato plants enhance the accumulation of osmolytes such as proline, which acts as a protective agent against osmotic imbalance, and secondary metabolites like polyphenols, which scavenge harmful ROS (Karakan et al., 2024). These compounds are considered key indicators of salt and alkaline tolerance (Rao et al., 2023; Aung et al., 2022). Additionally, non-protein amino acids such as γ-Aminobutyric acid (GABA) and key metabolites like glutamate, which is a precursor of GABA, enhance antioxidant defences, stabilize membranes, and maintain protein integrity under stress conditions (Assouguem et al., 2024; Xu et al., 2022; Wang et al., 2024). While these biochemical responses are well described for salinity, fewer studies have examined their roles in alkaline stress adaptation in tomato.

Furthermore, ionomic responses play a crucial role in stress tolerance. Elevated rhizosphere pH can reduce the availability of nutrients such as Ca^{2+}, Mg^{2+}, and phosphate, and excessive Na^{+} accumulation can disrupt K^{+} homeostasis, thereby impairing enzymatic functions and ion balance (Rao et al., 2023; Kaspal et al., 2021). Alkaline stress also alters rhizosphere microbial communities (Wu et al., 2021; Zhang et al., 2022a) and impacts nutrient cycling, further exacerbating stress effects on plants. However, the detailed ionomic responses of tomato under alkaline stress remain largely unexplored.

At the molecular level, plants respond to alkaline pH stress by activating complex signalling networks such as MAPK cascades, which regulate stress-responsive gene expression and interact with hormonal pathways including ethylene and ABA (Xu et al., 2022; Neina, 2019). In tomato, *SlMAPK3* and *SlACO1* (*ACC* oxidase, a key ethylene biosynthesis gene) have been shown to play critical roles in tolerance to alkaline stress; silencing these genes reduces ethylene production and impairs stress adaptation (Neina, 2019). A recent review also highlights the central role of MAPKs in coordinating stress signals and modulating downstream responses in tomato under both biotic and abiotic stresses, including saline-alkaline stress (Zhang et al., 2022b). Similarly, ethylene signalling has also shown to regulate oxidative stress responses and maintain cellular homeostasis under alkaline conditions in tomato (Shi et al., 2025). On the other hand, key transcription factors (TFs), including *MYB, WRKY, bZIP,* and *AP2/ERF*, along with signalling pathways such as *SOS,* and *CDPK*, coordinate the regulation of ion transporters, antioxidant systems, and osmolyte metabolism (Rao et al., 2023; Wang et al., 2024). Proton pump transporters like *SlHKT1;1* and *HKT1;2* play central roles in mediating Na^{+} transport and tissue distribution, contributing to ionic homeostasis under salinity and alkaline stress (Yang et al., 2024; Hu et al., 2024). However, the full molecular framework underlying genotype-specific alkaline stress tolerance in tomato needs deeper investigation.

Elucidating these pathways is essential for improving cultivars with adaption to high-pH soils. Here, we compared two contrasting tomato genotypes A10 (alkaline-tolerant) and M56 (alkaline-sensitive) subjected to NaOH-induced alkaline stress. Through integrative transcriptomic, biochemical, and ionomic analyses, we identified key regulatory networks and physiological traits that underpin tolerance. These findings provide valuable insights to guide breeding for alkaline stress-resilient tomato plants.

2. Materials and methods

2.1. Plant material and growing conditions

The plant material used in this study is a part of a collection from the Department of Agronomy, Food, Natural Resources, Animals, and Environment (DAFNAE) at the University of Padova (Italy). This includes A10 (highly tolerant) and M56 (sensitive), selected based on preliminary field screening for their responses to alkaline stress, showing significant yield differences (Supplementary S11, S12&S13) under alkaline conditions (soil pH $>$ 7), M56 exhibited chlorosis, leaf curling, reduced leaf expansion, and overall growth retardation. Seeds from both the varieties were initially soaked in 3 % hydrogen peroxide for 30 min to ensure disinfection (Sanna et al., 2022), followed by thorough rinsing with distilled water. Subsequently, they were placed into boxes containing moistened germination paper and kept in the dark at 25 °C until germination. After 3 days, seedlings were transferred to 500-mL glass pots containing a hydroponic nutrient solution (NS) in a growth chamber at 25 °C with a 16-h photoperiod with light intensity (PFD) of 400 μmol photons m^{-2} s^{-1}, relative humidity was kept constant at 60 %, sterilized cotton plugs as medium. The NS was a modified Hoagland and Arnon (1950) (Arnon, 1950) formulation, adjusted for tomato The composition per liter of solution was as follows: 7 mL of 1.4 M calcium nitrate tetrahydrate ($Ca(NO_3)_2{\cdot}4H_2O$), 5 mL of 1.4 M potassium nitrate (KNO_3), 2 mL of 0.28 M monopotassium phosphate (KH_2PO_4), 2 mL of 1.4 M magnesium sulfate heptahydrate ($MgSO_4{\cdot}7H_2O$), and 1 mL of 0.7 M FeEDTA. Additionally, 1 mL of a trace element stock solution was added, containing 0.322 M boric acid (H_3BO_3), 0.063 M manganese chloride tetrahydrate ($MnCl_2{\cdot}4H_2O$), 0.00252 M zinc chloride ($ZnCl_2$), 0.00602 M copper(II) chloride dihydrate ($CuCl_2{\cdot}2H_2O$), and 0.00077 M sodium molybdate dihydrate ($Na_2MoO_4{\cdot}2H_2O$). Plants were exposed to three different pH conditions: a control Hoagland solution (pH 5.9, EC 2.5 dS/m) and two alkaline stress conditions achieved by adjusting the pH of the Hoagland solution with NaOH to 8.2, EC 4.5 dS/m (1 mM NaOH) and to 9.2, EC 6 dS/m (1.5 mM NaOH). The pH of each solution was monitored using a digital pH-meter (Crimson BASIC 30, Crimson Instruments, Barcelona, Spain). The pH electrode was calibrated before each experiment, with the manufacturer specifying a measurement error of approximately ±0.05 pH units. The pH measurements were taken on daily basis, and adjustments were made as necessary using low concentrations either NaOH or HCl to maintain the same pH levels throughout the experiment. The NS was renewed every 4 days to maintain the same conditions throughout the experiment. After 10 days of growth, plants were transferred to 5-L boxes. Leaf samples were collected at different growth stages for various analyses: (1) Transcriptomic analysis was performed after 8 days of growth. (2) After 30 days of growth at the end of the BBCH-19 stage, leaf samples (3rd and 4th leaves from the top) were collected for biochemical analyses (*i.e.*, proline, polyphenols, and amino acid contents) and (3) after 45 days early BBCH-51 stage (and the 5th and 6th leaves from the top) for ionomics analysis.

2.2. RNA isolation

For transcriptome sequencing and RT-qPCR studies, fresh leaves and whole roots (rinsed with deionized water, dried with sterile filter paper) from each experimental condition were sampled 8 days after being moved to hydroponics with different pH conditions. Fifty mg of pooled samples leaf tissues from each replicate was frozen immediately using liquid nitrogen and subsequently stored at −80 °C until further processing. Frozen tissues were ground in liquid nitrogen using a tissue homogeniser and total RNA was extracted by using a Plant RNAeasy

MiniKit (Quiagen, USA) following the manufacturer's recommended protocol. The isolated total RNA quality and quantity were assessed using an Agilent Tape Station 1500 (Agilent Technologies Inc., Santa Clara, CA, USA).

2.3. Transcriptomic sequencing and data analysis

RNA-seq was performed with three biological replicates per genotype and condition (control pH 5.9, pH 8.2, and pH 9.2), ensuring statistical robustness for differential expression analysis. Each replicate consisted of pooled leaf tissues from independent plants grown under identical conditions. RNA samples were sequenced using the Illumina NovaSeq 6000 sequencing paired-end sequencing platform at Novogene GmbH with nearly 20 million reads per sample and a read length of 150bp. Raw paired-end reads were first analysed using FASTQC (Babraham Bioinformatics) for sequencing quality and then mapped onto the tomato reference genome SL4.0 downloaded from Phytozome V.13 (Goodstein et al., 2012; Hosmani et al., 2019) using Bowtie2 v2.3.5.1 (Langmead and Salzberg, 2012). Aligned SAM files were further processed using the Samtools suite (Li et al., 2009) and the gene feature counts matrix was generated by bedtoools multicov using ITAG 4.0 gene annotation file. iDEP.96 (Ge et al., 2018) was further used to analyse the count matrix to perform clustering and identify Differentially Expressed Genes (DEGs), which were considered by the criteria of their raw p-value <0.05 and $\log_2$(Fold Change) $| > 1$. The analysis compared the genetic expression profiles in the different experimental conditions to identify processes related to adaptation in alkaline environments by testing both genotypes in their optimum condition (pH = 5.9) against their alkaline-stressed situations (pH = 8.2 and 9.2). Identified DEGs have been analysed with the online software G:profiler (Raudvere et al., 2019) for Gene Ontology (GO) enrichment and KEGG pathways analyses.

2.4. RT-qPCR analysis

Genes of interest related to alkaline stress tolerance were selected for validation through RT-qPCR based on transcriptome analysis and existing literature. Primers were designed using the NCBI Primer-BLAST tool, utilizing the respective coding sequences (CDS) of the genes from ITAG 4.0 annotation (Ye et al., 2012). A list of these primers is provided in Supplementary Table S8. The RT-qPCR assay was conducted using a reaction mixture consisting of 5 μL of QuantiTect SYBR Green (Qiagen, Hilden, Germany), 0.1 μL of reverse transcriptase (Qiagen, Hilden, Germany), and 0.5 μL of each gene-specific primer. The average cycle threshold (Ct) values of the internal control gene were determined. Relative gene expression analysis was performed using the comparative $2^{-\Delta\Delta Ct}$ method (Schmittgen and Livak, 2008).

2.5. Biochemical analyses

Leaf samples for proline and polyphenol quantification were collected 30 days after the beginning of the experiment, with six biological replicates for each experimental condition.

Proline concentration was determined using the method outlined by Bates et al. (1973) and Quagliata et al. (2023) (Bates et al., 1973; Quagliata et al., 2023). Specifically, 0.1 g of fresh leaf tissue was homogenised in 2 mL of 3 % (w/v) 5-sulfosalicylic acid dihydrate and centrifuged at 5000 rpm for 10 min. The resulting supernatant was utilised to estimate proline content. The reaction mixture, consisting of 500 μL of supernatant, 500 μL of acetic acid, and 500 μL of acid-ninhydrin reagent, was boiled at 100 °C for 1 h and then cooled in an ice bath to block the reaction. The mixture was subsequently extracted with 1.5 mL of toluene, and the absorbance was measured at 520 nm with a UV–Vis spectrophotometer (8453, Agilent, Santa Clara, CA, USA), using toluene as a blank. Calibration was done with 2–600 μL of a 1 mM L-proline (98.5–101.0 %, pharma grade, PanReac AppliChem ITW Reagents S.R.L., Monza, Italy) stock solution. Proline concentrations were expressed as μmol g^{-1} fresh weight (FW).

The total polyphenol content (TPC) was assessed in extracts of tomato leaves, that had been dried in the dark, following the protocol suggested by Ghorbani et al. (2024) (Ghorbani et al., 2024). TPC was quantified using the Folin-Ciocalteu method (Al-Duais et al., 2009). Absorbance measurements of the samples were conducted at 760 nm using a UV–Vis spectrophotometer (8453, Agilent, Santa Clara, CA, USA). Gallic acid (98 %, Thermo Fisher Scientific Inc., Rodano, Milano, Italy) (in the 5–300 μg mL^{-1} concentration range) was the standard of choice. TPC was expressed as gallic acid equivalent (GAE) mg g^{-1} DW of extract.

The quantification of free amino acids (FAAs) was assessed in tomato leaves after 30 days of growth, using six biological replicates per condition, following the method described in Fedeli et al. (2023) (Fedeli et al., 2023) with slight modifications. Approximately 1 g of FW was homogenised in 2 mL of distilled water for 2 min and centrifuged at 4000 rpm for 5 min to obtain a clear extract. According to AccQ-Tag protocol (Waters Corporation, Milford, MA, U.S.A.), each reconstituted sample (10 μl) was amino acid derivatized with the AQC fluorescent reagent and 0.02 M borate buffer (pH 8.6) (Cohen and Michaud, 1993). This analysis was performed by using High-Performance Liquid Chromatography (HPLC) system (model LC1, Waters Corporation, Milford, MA, U.S.A.), equipped with a reversed-phase Zorbax 5 μm C18 column (4.6 × 250 mm, Agilent, Santa Clara, CA, U.S.A.), thermostatically regulated at 37 °C. Detection was facilitated by a Waters 470 scanning fluorescence detector with excitation set at 250 nm and detection at 395 nm. The mobile phase, flowing at a rate of 1.0 mL min^{-1}, consisted of two solvents: (A) 127 mM sodium acetate with 19 mM triethylamine titrated to pH 5.0 with phosphoric acid; (B) 60 % (v/v) acetonitrile in water, with the gradient elution indicated in Table 1. Quantification of each amino acid was estimated by matching the area under the peak of the chromatogram to the amino acid standard (WAT088122, Waters Corporation, Milford, MA, U.S.A.), using the OpenLab ChemStation software (Chromatography Data Systems, Agilent, Santa Clara, CA, U.S.A.).

2.6. Leaf ionomics analysis

Leaves were sampled at BBCH 51, 45 days after planting, from both tolerant and susceptible genotypes grown under varying pH conditions to investigate the influence of genotype and pH on element uptake. Six biological replicates were collected for each experimental condition. The leaves were dried overnight at 95–100 °C, with each sample weighing approximately 1.5 g. After drying, the leaves were digested with nitric acid (HNO_3), and elemental concentrations were measured using inductively coupled plasma optical emission spectrometry (ICP-OES). Elemental quantification was performed with certified multi-element standards, and the results were expressed in mg.kg^{-1} of dry matter. The analysis covered the following elements: Al, As, B, Ba, Be, Ca, Cd, Co, Cr, Cu, Fe, Hg, K, Li, Mg, Mn, Mo, Na, Ni, P, Pb, S, Sb, Se, Sn, Sr, Ti, Tl, V, and Zn. This methodology was adapted from Thakare et al.

Table 1
Gradient elution used for the separation of FAAs.

Time (min)	Flow rate (mL min^{-1})	Mobile phase (%)	
		A	B
0.84	1.0	98	2
25	1.0	93	7
31.7	1.0	90	10
53.4	1.0	67	33
55.1	1.0	67	33
56.8	1.0	67	33
61.8	1.0	75	25
63.5	1.0	100	0
70	1.0	100	0

(2024) (Thakare et al., 2024).

2.7. Calculation of Alkaline Tolerance Index (ATI)

To quantify the relative tolerance of each genotype to alkaline stress, an Alkaline Tolerance Index (ATI) was calculated for key physiological and biochemical traits. The ATI was defined as the ratio of the mean value of a given trait under alkaline stress conditions (pH 8.2 and pH 9.2) to the mean value under control conditions (pH 5.9), following the general approach of stress tolerance indices described by Fischer and Maurer (1978) (Fischer and Maurer, 1978) and adapted for saline-alkaline stress by Rao et al. (2023) and Aung et al. (2022) (Rao et al., 2023; Aung et al., 2022), to standardize genotype comparisons under alkaline stress. Similar ratio-based metrics (e.g., K^+/Na^+, Stress Tolerance Score) have been validated in recent studies of saline-alkaline responses (Shang et al., 2024; Abdelmoneim et al., 2025). While ATI provides a quantitative framework for cross-trait comparisons, its thresholds are context-dependent and should be interpreted alongside mechanistic data (e.g., ion transport, ROS scavenging).

ATI = (Trait value under alkaline stress) / (Trait value under control)

Where an ATI value > 1 indicates an increase under stress (potential adaptive response), while ATI <1 suggests a reduction in the trait under stress.

2.8. Statistical analyses

A two-way analysis of variance (ANOVA) was conducted to evaluate the effects of genotype, conditions, and their interaction on the measured variables. Statistical significance was determined at $p \leq 0.05$. To control for false discovery rate (FDR), adjusted p-values (*p adj)* were used in relevant comparisons, while unadjusted p-values were applied for general exploratory analyses. Post hoc comparisons among means were performed using Tukey's Honest Significant Difference (HSD) test and Duncan's Multiple Range Test (MRT) to delineate homogeneous groups. All analyses were conducted using R Studio (RStudio Team, 2025).

3. Results

3.1. Transcriptomics

Transcriptomic analysis was conducted on 8-day-old seedlings subjected to alkaline stress conditions. This time point was chosen because it represents a critical early developmental stage when seedlings exhibit high metabolic activity and plasticity, allowing for the detection of immediate molecular responses before the onset of severe or irreversible stress symptoms. Principal component analysis (PCA) and Venn diagram analysis together revealed distinct and genotype-dependent transcriptomic responses to alkaline stress (Fig. 1A and B). PCA showed a clear separation of transcriptomic profiles between conditions and genotypes. The first component (PC1), accounting for 64.1 % of total variance, captured the impact of increasing pH, while PC2 (12.5 %) highlighted genotype-specific responses. Notably, A10 exhibited a broader transcriptional shift at pH 9.2, suggesting a more robust transcriptional reprogramming under severe alkaline conditions. Complementing this, Venn diagram analysis revealed that A10 differentially expressed 556 genes at pH 8.2 vs. pH 5.9 (control) and 389 genes at pH 9.2 vs. pH 5.9 (control) (L2FC > 1; $p < 0.05$). In contrast, the M56 genotype showed minimal transcriptional changes, with only 20 and 44 DEGs at the same comparisons, respectively (L2FC > 1; $p < 0.05$).

Gene ontology analysis on the two comparisons in both genotypes. Only the 15 most enriched Biological Processes (BP) have been considered in each comparison (*p adj* < 0.05; -log10(*p adj*) < 1). In the A10 genotype at pH 8.2 compared to the control, 140 genes out of the 556 DEGs were causative for the most significantly enriched BP and were related to biological and cellular processes such as biological regulation, signalling, response to chemical stimulus (Supplementary Fig. S1 and S2). While at pH 9.2, 20 genes out of the 389 DEGs were causative for enriched BP. Apart from the observed BP at pH 8.2 with response to ethylene at pH 9.2 (Supplementary Table S1). At pH 8.2 and pH 9.2 compared to the control, the most significantly enriched BP was related to response to stimuli. At pH 8.2 in the M56 genotype, 5 genes out of the 20 DEGs were causative for enriched BP and were mostly related to the response to light, photosynthesis, transport of malate, organic acid, Na ion transportation and signalling (Supplementary Fig. S3 and S4). Six genes out of the 44 DEGs were causative for these

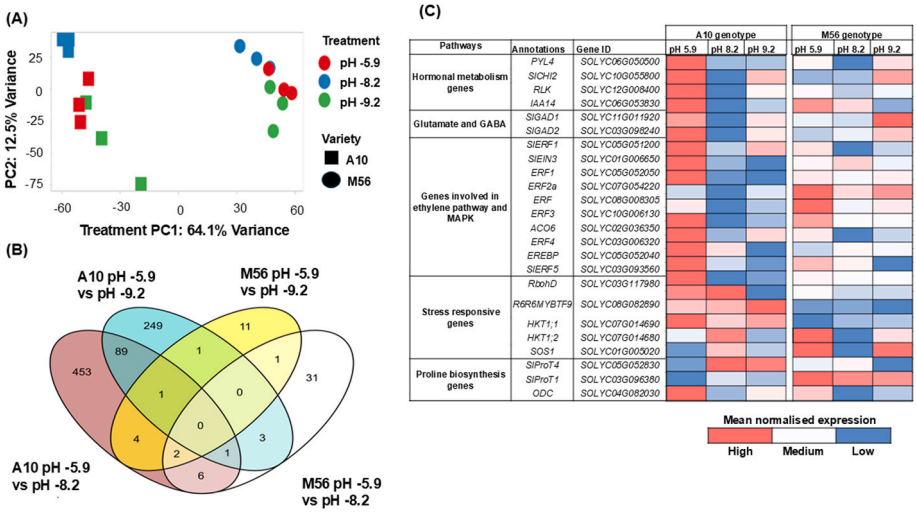

Fig. 1. (A) Principal Component Analysis (PCA) plot illustrating the clustering of samples under different alkaline conditions representing in different colours within the tolerant (A10) in (squares shape) and susceptible (M56) genotypes (circular shape). Clustering within each genotype indicates stable transcriptional responses to pH, supported by PERMANOVA showing significant genotypic differences ($p = 0.001$). (B) Venn diagram depicting the number of differentially expressed genes (DEGs) shared across pH conditions. The overlap represents common DEGs at pH 8.2 and pH 9.2 compared to the control (pH 5.9) in A10 and M56, highlighting both genotype-specific and shared transcriptional responses. (C) Mean normalised expression profiles of genes at pH 8.2 and pH 9.2 relative to the control (pH 5.9) in A10 and M56, showing overall gene expression trends under alkaline stress. (For interpretation of the references to colour in this figure legend, the reader is referred to the Web version of this article.)

enriched BP at pH 9.2. The most significant BP for the M56 genotype was related to the regulation of circadian rhythms, cell growth, and amine catabolism (Supplementary Tables S2 and S3).

KEGG pathways analysis on the two comparisons in both genotypes. The most enriched KEGG pathways have been considered in each comparison ($p\ adj < 0.05$; -log10($p\ adj < 1$). In the A10 genotype, 31 genes out of the 556 DEGs were causative for enriched pathways (Supplementary Fig. S5), while at pH 9.2, 32 genes out of the 389 DEGs were causative for enriched pathways. This genotype showed amino acid-related pathways significantly enriched exclusively at pH 8.2 (Supplementary Tables S4 and S5, Supplementary Fig. S6) and at pH 9.2 significant hormonal pathways. At both pH 8.2 and pH 9.2 compared to the control pH 5.9, KEGG highlighted the MAPK signalling pathway, biosynthesis of secondary metabolites, plant hormone signalling cascades, and interactions between plants and pathogens. At pH 8.2, the M56 genotype showed only 4 KEGG pathways enriched (Supplementary Table S6 c, Supplementary Fig. S7). Only three genes out of the 20 DEGs were causative for these enriched pathways. At pH 9.2 (Supplementary Table S7 c, Supplementary Fig. S8). Six genes out of the 44 DEGs were causative for these enriched BP. Differential gene expression analysis between conditions identified multiple DEGs, as illustrated in Fig. 1C.

3.2. RT-qPCR validation of genes of interest

The expression profiles of *Solanum lycopersicum* genes *SOS1, SlHKT1;1, and SlHKT1;2* were analysed in the leaves and roots of the tolerant genotype (A10) and the sensitive genotype (M56) following 8 days of alkaline stress (pH 8.2 and pH 9.2) under hydroponic conditions (Fig. 2). In leaf tissue, *SOS1* expression was significantly upregulated under both pH 8.2 and pH 9.2 in A10 ($p\ adj = 0.0396$, $p\ adj = 0.0019$) and under pH 8.2 in M56 ($p\ adj = 0.0336$) with respect to control condition. In contrast, a significant downregulation of *SOS1* was observed in the roots of A10 under pH 9.2 ($p\ adj = 0.0374$) (Fig. 2A and B), indicating a tissue and genotype-specific transcriptional response. *SlHKT1;1* expression was significantly elevated in the roots of M56 under pH 9.2 ($p\ adj = 0.0087$), with minimal increase under pH 8.2 ($p\ adj = 0.0563$). No significant changes in expression of *SlHKT1;1* were observed in A10 under either condition (Fig. 2C and D).

In A10, *SlHKT1;2* expression was significantly upregulated in leaves under both pH 8.2 and pH 9.2 ($p\ adj = 0.0117$, $p\ adj = 0.0000043$), and in roots under pH 9.2 ($p\ adj = 0.0015$). There are no significant changes in *SlHKT1;2* expression in M56 at pH 8.2 ($p\ adj = 0.0811$), but slightly higher than control (Fig. 2E and F). The expression of several genes involved in key metabolic and stress-response pathways was analysed. These included genes associated with glutamate and GABA metabolism, such as *glutamate decarboxylase* (*SlGAD1*, *SlGAD2*); ethylene biosynthesis genes, including *1-aminocyclopropane-1-carboxylic acid synthase* (*ACS*, *ACS2*); drought tolerance, such as *respiratory burst oxidase homolog 1* (*RbohD*); and abiotic stress responses, such as *R2R3MYB transcription factor 9;* Class II chitinases, like *CHI2; SlPYL4*, an ABA receptor. Among these, *SlGAD1* was significantly induced in A10 under both pH 8.2 and pH 9.2 ($p\ adj = 0.0421$, $p\ adj = 0.000062$), as was *SlGAD2* ($p\ adj = 0.0000227$, $p\ adj = 0.0012$) in leaves (Supplementary Fig. S9A and B). The transcription factor *R2R3MYB9* was strongly upregulated in the leaves of A10 under both pH 8.2 and pH 9.2 ($p\ adj = 0.0009$, $p\ adj = 0.0118$) (Supplementary Fig. S9D). Additionally, *ACS2*, an ethylene biosynthesis gene, was significantly induced in A10 under pH 9.2 ($p\ adj = 0.0013$), with a marginal increase under pH 8.2 ($p\ adj = 0.0561$) (Supplementary Fig. S9E).

3.3. Effects of alkaline stress on proline and polyphenol accumulation

In this study, proline content was assessed in two tomato genotypes subjected to increasing alkalinity levels (Fig. 3A). The results showed that alkaline pH condition significantly affected proline accumulation in the leaves ($p < 0.05$). In the A10 genotype, proline content increasing trend at pH 8.2 (17.4 %) and even more at pH 9.2 (36.92 %); conversely, in the M56 genotype, proline content was reduced of 26.56 % at pH 8.2 and even reduced of 37.67 % at pH 9.2, compared to the control (Fig. 3A). Notably, no differences were observed in proline content

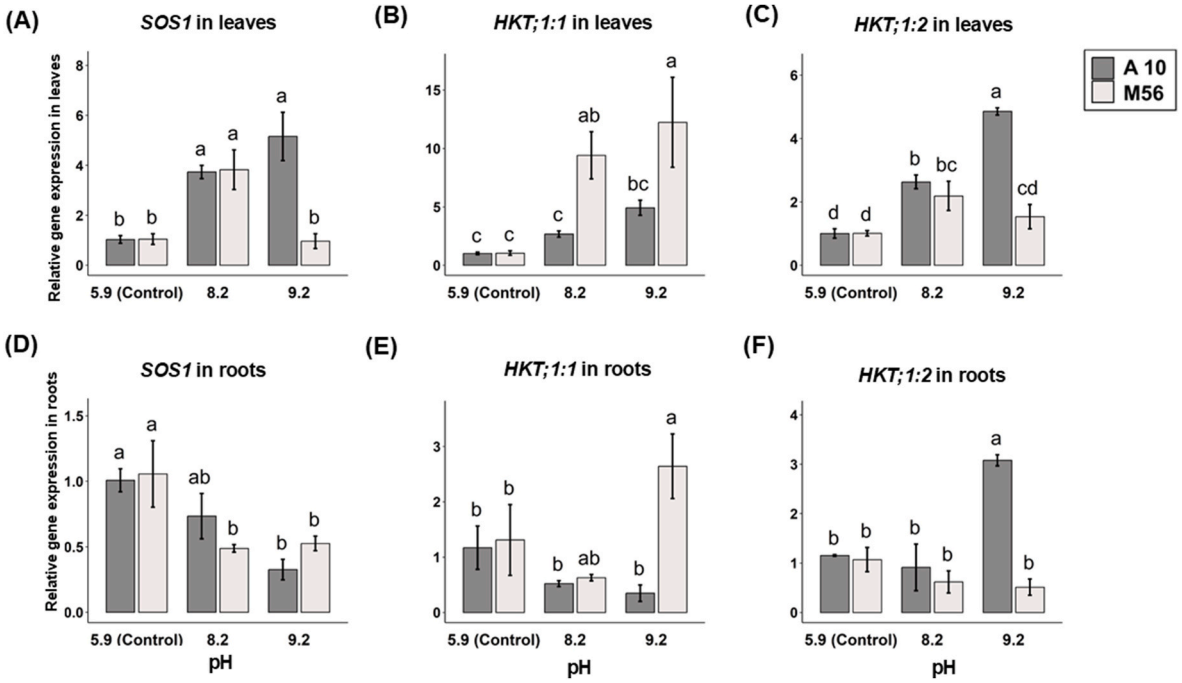

Fig. 2. The expression levels of (A) SOS1 in leaves, (B) HKT1; 1 in leaves, (C) HKT1; 2 in leaves, (D) SOS1 in roots, (E) HKT1; 1 in roots, and (F) HKT1; 2 in roots were analysed in tomato genotypes A10 and M56. Tomato α-tubulin (TUA) was used as the reference gene. Expression changes were evaluated in response to alkaline stress conditions (pH 5.9, 8.2, and 9.2). Data are presented as mean ± SE (n = 9), representing three biological and three technical replicates. Statistical significance was determined by two-way ANOVA followed by Tukey's HSD post hoc test ($p \leq 0.05$). Different letters denote significantly different groups based on Duncan's multiple range test.

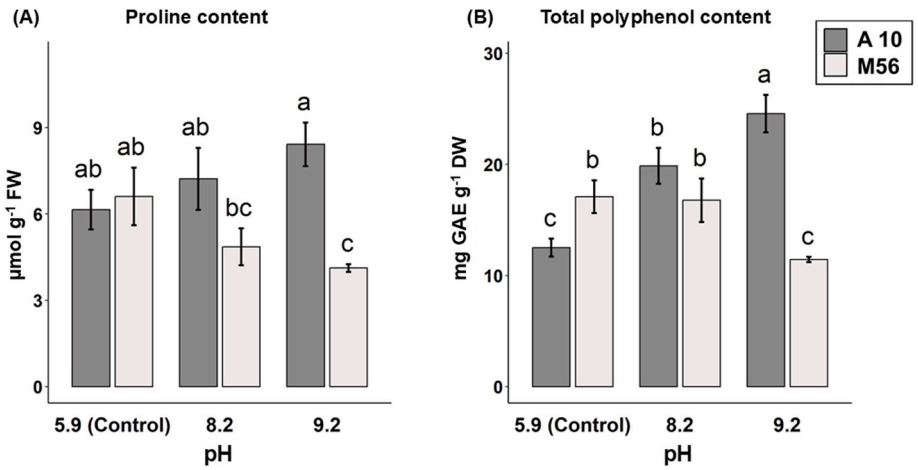

Fig. 3. (A) Proline content and (B) total polyphenol content (TPC) in the leaves of tomato genotypes A10 and M56 after 30 days of treatment under control (pH 5.9) and alkaline stress conditions (pH 8.2 and pH 9.2). Data are presented as means ± SE (n = 6). Statistical significance was determined using two-way ANOVA followed by Tukey's HSD post hoc test ($p \leq 0.05$). Different letters indicate significantly different groups according to Duncan's multiple range test.

between the two genotypes under control conditions (pH 5.9). However, more pronounced differences were evident between the two genotypes at pH 8.2 and pH 9.2 (Fig. 3A).

The TPC in the A10 genotype increased significantly and progressively with rising alkalinity levels (Fig. 3B). Specifically, there was an increase at pH 8.2 (58.81 %) ($p\ adj = 0.007$) and an even higher increase at pH 9.2 (96.42 %) ($p\ adj = 0.00001$). In contrast, TPC in the M56 genotype showed a decreasing trend in response to increasing alkalinity, with a sharp reduction at pH 9.2 (33.06 %) (Fig. 3B). The differences in TPC between the two genotypes are statistically significant ($p < 0.05$) in control conditions (pH 5.9) and at the highest alkalinity condition (pH 9.2).

3.4. Effects of alkaline stress on FAA analysis

The total content of FAAs, as well as the contents of individual amino acids in both genotypes, fluctuated along with the increasing alkalinity conditions in both genotypes. Amino acids of the A10 genotype clustered differently from amino acids of the M56 genotype (Fig. 4A). In the A10 genotype, total FAA content increased slightly at pH 8.2 (16 %) and more at pH 9.2 (26.89 %); in the M56 genotype, FAAs content increased (65.56 %) at pH 8.2 but then decreased (38.24 %) at pH 9.2, compared to the control (Fig. 4B). A significant genotypic difference in free amino acid (FAA) content was observed under pH 9.2 conditions ($p\ adj = 0.0025$).

Furthermore, alkaline conditions modulated the accumulation of several amino acid. Specifically, aspartate content in A10 increased by 28.46 % at pH 8.2 and 47.3 % at pH 9.2, and in M56 increased by 85.34 % at pH 8.2 and decreased by 41.57 % at pH 9.2 (Fig. 5A), GABA content in A10 increased by 25.46 % at pH 8.2 and 7.30 % at pH 9.2, and in M56 increased by 66.46 % at pH 8.2 and decreased by 48.30 % at pH 9.2 (Fig. 5B), glutamate content in A10 raised by at pH 8.2 37.30 % and 49.46 % at pH 9.2, and in M56 increased by 125 % at pH 8.2 and decreased by 30.52 % at pH 9.2 (Fig. 5C), serine content in A10 increased by 26.47 % at pH 8.2 and 69.91 % at pH 9.2, and in M56 increased by 51.47 % at pH 8.2 and decreased by 38.91 % at pH 9.2 (Fig. 5D), lysine content showed no variation at pH 8.2 but increased by 63.23 % at pH 9.2, and in M56 increased by 74.29 % at pH 8.2 and decreased by 14.21 % at pH 9.2 (Fig. 5E), and leucine content increased by 12.90 % at pH 8.2 and 21.29 % at pH 9.2, and in M56 a slight increase of 8.7 % at pH 8.2, but a decrease of 48.48 % at pH 9.2 (Fig. 5F), compared to the control in the leaves of A10 and M56 genotypes.

The results demonstrated that alkaline stress affected the content of various FAAs in the leaves of both genotypes ($p \leq 0.05$). A trend of increment in FAAs with raising alkaline stress conditions was observed with the A10 genotype, whereas in M56 genotype FAAs increased at pH 8.2 but showed a sharp decline at pH 9.2.

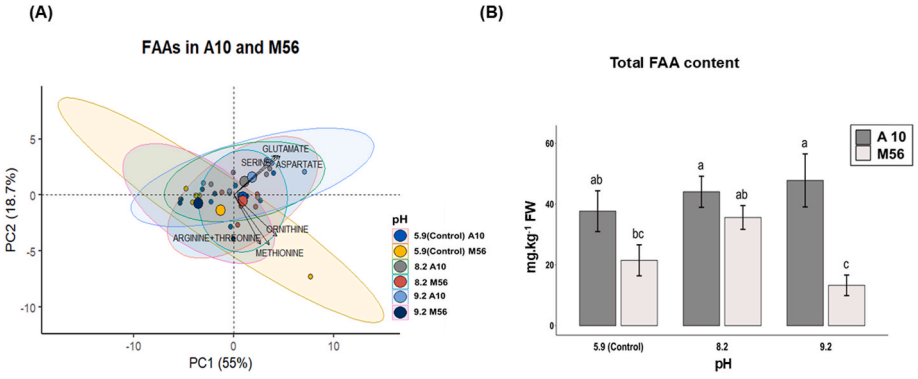

Fig. 4. (A) Principal Component Analysis (PCA) of free amino acids (FAAs) and (B) total FAA content in the leaves of tomato genotypes A10 and M56 after 30 days of treatment under control (pH 5.9) and alkaline stress conditions (pH 8.2 and pH 9.2). Data are presented as means ± SE (n = 6). Statistical significance was assessed using two-way ANOVA followed by Tukey's HSD post hoc test ($p \leq 0.05$). Different letters indicate significantly different groups based on Duncan's multiple range test.

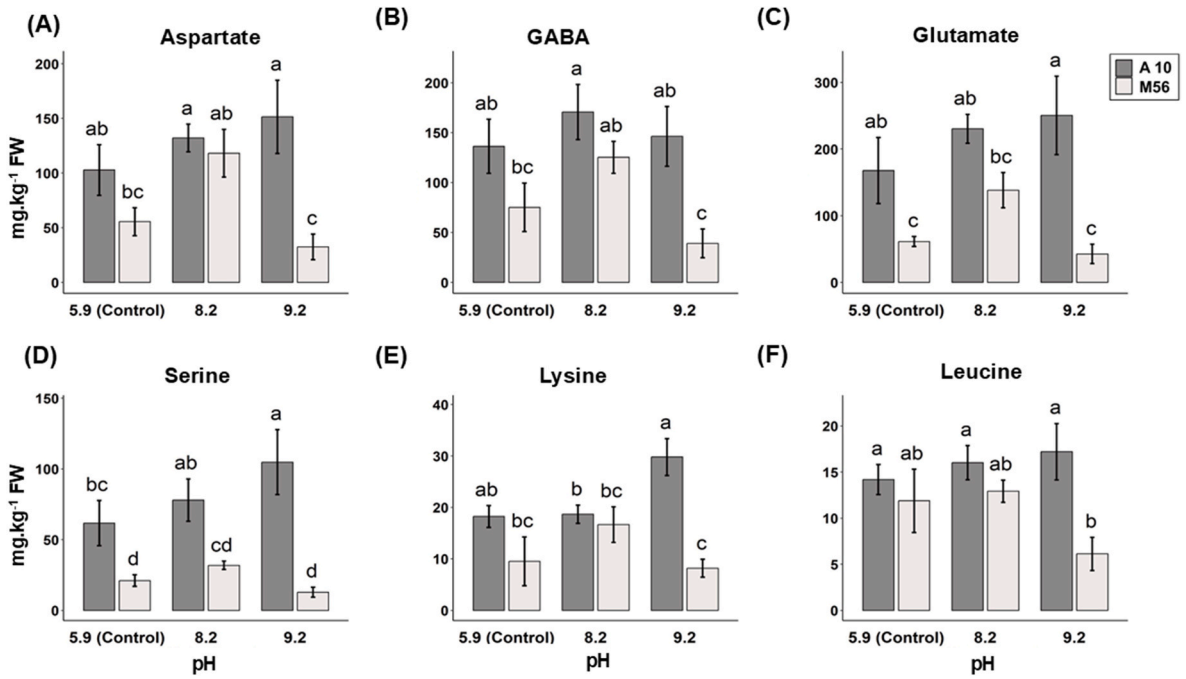

Fig. 5. Content of different free amino acids (FAAs) was measured in the leaves of tomato genotypes A10 and M56 after 30 days of treatment under control (pH 5.9) and alkaline stress conditions (pH 8.2 and pH 9.2). The analysed FAAs include (A) aspartate, (B) GABA, (C) glutamate, (D) serine, (E) lysine, and (F) leucine. Data are presented as means ± SE (n = 6). Statistical significance was determined using two-way ANOVA followed by Tukey's HSD test ($p \leq 0.05$). Different letters denote significantly different groups according to Duncan's multiple range test.

3.5. Effects of alkaline stress on leaf ionomics analysis

Leaf ionomics, performed under different pHs (5.9 = control, 8.2, and 9.2) with 6 replicates per condition, revealed significant differences in elemental composition between the two genotypes (Fig. 6). In A10, Na content significantly rose by 405.2 % at pH 8.2 ($p\ adj = 0.0003$), and 299.97 % at pH 9.2 ($p\ adj = 0.01$), while, in M56, it increased significantly with a 565.0 % rise at pH 8.2 ($p\ adj = 0$), and 809.3 % at pH 9.2 ($p\ adj = 0$), compared to the control (pH 5.9). In M56, Na content was roughly twice that of A10 at pH 8.2 and pH 9.2 (Fig. 6A). In A10,

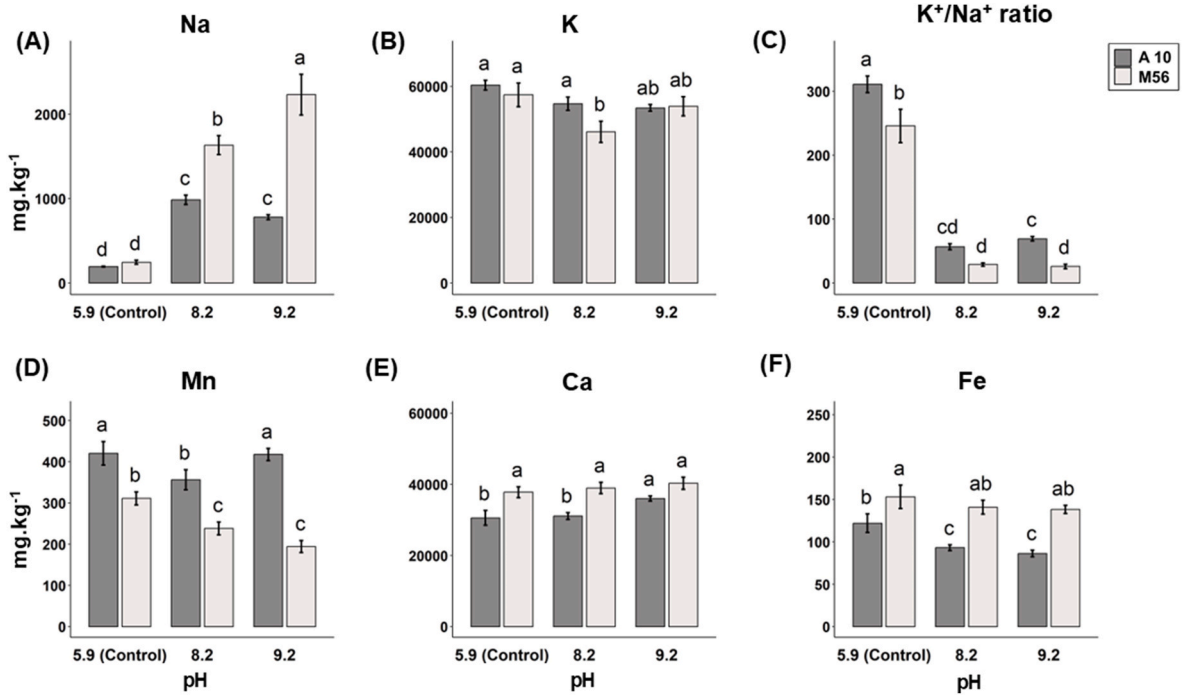

Fig. 6. The content of different elements was measured in the leaves of A10 and M56 genotypes after 45 days of treatment, including a control (pH 5.9) and two alkaline conditions (pH 8.2 and pH 9.2). The analysed elements included: (A) sodium (Na), (B) potassium (K), (C) K^+/Na^+ ratio, (D) manganese (Mn), (E) calcium (Ca), and (F) iron (Fe). Data are expressed as means ± SE (n = 6). Statistical significance was determined using two-way ANOVA followed by Tukey's HSD test ($p \leq 0.05$). Different letters denote significantly different groups according to Duncan's multiple range test.

potassium (K) content decreased slightly by 9.35 % at pH 8.2 and by 11.48 % at pH 9.2, while, in M56, it exhibited a decline of 19.63 % at pH 8.2 and a slight decrease of 6.09 % at pH 9.2 (Fig. 6B). K^+/Na^+ ratios declined sharply in both genotypes under stress, with A10 showing a decrease of 82.05 % at pH 8.2 and 77.86 % at pH 9.2, and M56 dropping further: 87.91 % at pH 8.2 and 89.67 % at pH 9.2 (Fig. 6C).

In A10, manganese (Mn) slightly fluctuated by 15.26 % at pH 8.2 and 0.65 % at pH 9.2, while M56 showed a consistent decrease by 23.4 % at pH 8.2 and 37.5 % at pH 9.2 (Fig. 6D). In A10, calcium (Ca) content remained stable at pH 8.2 and increased at pH 9.2 (18.1 %), whereas M56 remained constant under any imposed alkaline stress conditions (Fig. 6E). Finally, iron (Fe) content fluctuated slightly in both genotypes; in A10, it decreased substantially by 23.6 % at pH 8.2 and by 29.4 % at pH 9.2 compared to their controls. A similar decreasing trend was also observed for M56 genotype, with Fe content decreased by 8.2 % at pH 8.2 and by 9.4 % at pH 9.2 compared to the control. However, Fe levels remained consistently 50 % higher in M56 compared to A10 (Fig. 6F). Ion homeostasis differed markedly between the two tomato genotypes across increasing alkaline conditions. For the sensitive genotype M56, sharp reductions in the K^+/Na^+, Ca^{2+}/Na^+, and Mg^{2+}/Na^+ ratios were observed with increasing pH (*ANOVA*, $p < 0.05$). In contrast, the tolerant genotype A10 maintained comparatively stable ion ratios across conditions, with changes in K^+/Na^+ ($p = 0.028$), Ca^{2+}/Na^+ ($p = 0.047$), and Mg^{2+}/Na^+ slightly higher but not statistically significant (Supplementary Table S15). Overall, these results highlight clear genotype-specific ion homeostasis patterns under alkaline stress, with M56 tending to accumulate higher Na, Ca, and Fe contents, while A10 exhibited greater stability in K and especially Mn contents across the tested pH levels.

3.6. Alkaline Tolerance Index (ATI)

To complement physiological, biochemical and transcriptomic observations, an Alkaline Tolerance Index (ATI) was calculated for key osmolytes and ion ratios to quantify genotype-specific adaptability under alkaline stress (Supplementary Table S16). The ATI analysis revealed consistent differences between the two genotypes. In the tolerant A10 genotype, proline, GABA, and total free amino acids (FAAs) showed ATI values greater than 1 at both pH 8.2 and pH 9.2, indicating active trait upregulation under increasing alkalinity. For example, A10 reached a proline ATI of 1.35 ± 0.08 and GABA ATI of 1.29 ± 0.07 at pH 9.2, confirming balanced osmotic adjustment. In contrast, the sensitive M56 genotype displayed declining ATI values for proline and FAAs, with proline dropping to 0.88 ± 0.05 at pH 9.2, indicating limited adaptive capacity. Ion homeostasis analysis showed A10's superior K^+/Na^+ regulation, with ratios remaining stable (0.95 ± 0.02 at pH 8.2 to 0.92 ± 0.03 at pH 9.2; ns), while M56 exhibited significant decline (0.78 ± 0.05 to 0.63 ± 0.06; $p < 0.01$). This aligns with A10's higher overall mean ATI (1.23 ± 0.04 vs M56's 0.87 ± 0.03 at pH 9.2)

4. Discussion

4.1. The MAPK-ethylene crosstalk is strongly associated with response to alkaline stress

The mitogen-activated protein kinase (MAPK) cascade is one of the main pathways to sense alkalinity-induced osmotic stress (Shah et al., 2021). The "MAPK signalling pathway – plant" KEGG pathway (KEGG:04016) was the most significantly enriched KEGG pathway at pH 8.2 compared to pH 5.9 (control) in the A10 genotype ($p\ adj = 0.001$; -log10($p\ adj$) = 2.747), and was also a relevant pathway in the A10 genotype at pH 9.2 compared to pH 5.9 (control) ($p\ adj = 0.071$; -log10($p\ adj$) = 1.50). Six genes (*SlEIN3, RbohD, SlERF1, PYL4, SlCHI2, RLK*) were highlighted in this pathway, and they were differentially expressed only in the A10 genotype under one or both conditions (Fig. 1C). Consistent with the literature, the genes listed in Supplementary Table S9, which belong to the MAPK pathway, are modulated in response to osmotic stress, leading to the accumulation of compatible solutes to reestablish osmotic balance in the cell (Fischer and Maurer, 1978). Moreover, the BP "Cellular response to ethylene stimulus" (GO:0071369) and "Ethylene-activated signalling pathway" (GO:0009873) resulted in significant enrichment in the A10 genotype at pH 9.2. Ten genes in the DEGs dataset have been selected since they are involved in ethylene metabolism (Supplementary Table S10). In the ethylene-related pathways, *EIN3/EIL* was overexpressed in the A10 genotype at pH 8.2 (L2FC = 1.770) and even more at pH 9.2 (L2FC = 2.282), but it showed no response in the M56 genotype. This gene has been reported to improve stress tolerance in Arabidopsis (Zhang et al., 2011) and sorghum (Wang et al., 2023) by mitigating ROS accumulation (Peng et al., 2014). In mulberry, EIN3/EIL also supports osmotic stress resilience by regulating ethylene biosynthetic genes (Liu et al., 2019). ERF1 was upregulated in A10 at pH 8.2 (L2FC = 1.656) but did not respond under other conditions. It is known to contribute to stress tolerance in Arabidopsis (Cheng et al., 2013) and broccoli, where it reduces ROS by promoting proline production and activating CAT, POD, and SOD antioxidant enzymes (Jang et al., 2018). Additionally, *RbohD* was overexpressed in A10 at both pH 8.2 (L2FC = 1.392) and pH 9.2 (L2FC = 1.310). This gene plays a role in stress responses across many plants, including tomatoes (Raziq et al., 2022), and is crucial for ROS production through NADPH oxidase (*RbohD*) during stress (Pi et al., 2018). Specifically, *RbohD* is responsible for stomatal closure under stress in tomato leaves (Chapman et al., 2019). *SlPYL4*, an ABA receptor, was also overexpressed in A10 at pH 8.2 (L2FC = 1.300) and pH 9.2 (L2FC = 1.287). This gene initiates the MAPK response, which confers stress resistance by counteracting ROS production (Wang et al., 2020b). Additionally, chitinase gene *CHI2* (L2FC = 2.448), overexpressed in A10, has been shown to increase salt resistance in maize and tobacco (Liu et al., 2020). Class II chitinases, like *CHI2* and *pcht28*, are linked to osmotic stress resistance (Chen et al., 1994). Most genes in the ethylene pathway, including *ERF2, ERF3*, and *ERF4,* were upregulated in A10 at pH 8.2 or 9.2. These genes are known to confer drought tolerance in poplar (Chen et al., 2022), salt tolerance in soy and wheat (Zhang et al., 2009; Rong et al., 2014), and in sweet potato and Arabidopsis (Yu et al., 2020). *SlERF5* is particularly important for stress tolerance in tomato (Pan et al., 2012), and its wild relative *Solanum chilense* (Gharbi et al., 2017). Ethylene production, regulated by *ACO* (*1-Amino-cyclopropane-1-Carboxylic Acid Oxidase*), stimulates *EIN3/EIL*, which in turn activates *RBOH* for ROS signalling (Khan et al., 2023), initiating a MAPK cascade. This cycle also activates *ERFs*, promoting enzymatic (like CAT, APX, POD, GR, SOD) and non-enzymatic antioxidants (like polyphenols), leading to ROS scavenging and improved salt tolerance (Jang et al., 2018). Khan et al. (2023) (Khan et al., 2023) proposed that increased NaCl levels trigger the MAPK cascade, leading to ethylene production through *ACS, ACC*, and *ACO*. Overexpression of these genes in crops increases alkaline resistance, and, in A10, all were overexpressed except *ACS* and *ACC*. *ERFs* regulates K^+/Na^+ homeostasis and antioxidant enzyme expression, contributing to ionic balance under stress (Wei et al., 2024). These findings are consistent with recent evidence that the SlWRKY80-mediated jasmonic acid pathway contributes to Na^+/K^+ homeostasis under saline-alkaline stress (Shang et al., 2024), further highlighting the central role of ion transport regulation in enhancing tolerance, as demonstrated by the favourable K^+/Na^+ ratios observed in the tolerant A10 genotype in this study. A10 also showed significantly lower Na content in its leaves in comparison with M56 genotype. Overall, although much of this regulatory network has been studied primarily in the context of salinity and drought, our findings suggest that these genes play a similar role in osmotic adjustment and ionic homeostasis under alkaline stress. Despite these findings, the molecular network for stress responses remains complex, and the roles of *ERFs* in ion homeostasis under alkaline stress need further investigation.

4.2. The antioxidant response to alkaline stress is a part of innate tolerance

Proline content rose with increasing alkalinity in the leaves of the A10 genotype, *vice versa* it decreased in the leaves of the M56 genotype (Fig. 3A). Proline can be produced through different pathways; one of these involves the transformation of aspartate into lysine, of lysine into glutamate, and finally of glutamate into proline (Wang et al., 2022). These three amino acids, precursors of proline, have all been quantified and showed increased content in A10 but not in M56 (Fig. 4). Proline can also be produced by using methionine and ornithine as precursors (Meena et al., 2019), but both these amino acids show no pattern in respect to the condition in both genotypes (Fig. 4). Thus, the preferred pathway used in the A10 genotype is the one starting from aspartate. Generally, proline increases with increasing alkalinity. Under alkaline stress, ROSs cause oxidative stress, and tolerant genotypes have a higher content of antioxidant compounds, working together with the detox system (Aung et al., 2022) Indeed, the A10 exhibited not only higher levels of proline but also increased TPC in comparison with M56 genotype (Fig. 3B). Polyphenols have a vital role in plants, contributing to cell wall structuring, modulating growth and development, and providing defence against both biotic and abiotic stressors (Abdelmoneim et al., 2025). This biochemical parameter showed an increased trend in A10 genotype under alkaline conditions, whereas a slight declining trend was observed in M56 with increasing alkalinity. These changes in phenolic content may result from the dual inhibitory and stimulatory impact of abiotic stress on phenolic acid biosynthesis (Sharma et al., 2019).

4.3. The FAA metabolism in response to alkaline stress

FAAs play a key role in plant growth, development, and response to stressors (Yu and Wang, 2016; Wang et al., 2015). The accumulation of amino acids, such as aspartate, glutamine, glutamate, GABA, and serine can impact osmotic adjustment under stress (Gzik, 1996; Li et al., 2015). This is consistent with previous studies by Li et al. (2015), Ji et al. (2016) and Yang et al. (2012) (Li et al., 2015; Ji et al., 2016; Yang et al., 2012). Glutamate decarboxylase (GAD) is responsible for transforming glutamate into GABA, a process crucial for GABA production and stress response (Shelp et al., 2021). *GAD1* and *GAD2* play significant roles in saline alkaline stress response and tolerance (Mishra et al., 2023), with *gad1/2* mutants unable to convert glutamate to GABA, making them oversensitive to salinity (Shelp et al., 2021). *SlGAD1* and *SlGAD2* were both upregulated only in the A10 genotype at pH 8.2 (Fig. 1C), (Supplementary Table S11). This is coherent with our amino acid profiling, which showed increasing levels of both glutamate and GABA with rising pH (Fig. 5B and (C)

Exogenous GABA application has been linked to reduced ROS levels, improved membrane stability, and enhanced phytohormone crosstalk. Many plant GADs contain a Ca^{2+}/calmodulin-binding domain, which activates GAD in response to stress-induced cytosolic Ca^{2+}/CaM complexation or proton (H^+) signals (Kaspal et al., 2021; Shelp et al., 2021).In the A10 genotype, GADs were overexpressed at pH 8.2, leading to maximum GABA accumulation, but GAD activity was undetectable at pH 9.2 despite increased glutamate (Fig. S9 A and B). High GABA levels are critical for stress adaptation (Zhang et al., 2022c), as GABA synthesis regulates pH, activates the GABA shunt and tricarboxylic acid cycle, which regulates NADPH oxidase activity and lowers ROS accumulation (Mishra et al., 2023). Exogenous GABA alleviates alkaline stress by regulating organic acid accumulation, linking the glycerate pathway to the GABA shunt (Wu et al., 2020; Ramos-Ruiz et al., 2019). Serine (Ser), synthesized through the glycerate and phosphorylated L-Ser biosynthesis pathways, serve as a precursor for glycine, formate, and glycolate, all of which tend to accumulate under stress conditions. These pathways are hypothesised to regulate redox balance in stressed plants, emphasizing the essential role of carbon and nitrogen metabolism in maintaining cellular redox and energy levels (Igamberdiev and Kleczkowski, 2018).

FAAs showed a increasing trend in both genotypes with the increased level of alkaline stress. A10 had maximum value for amino acids as compared to M56 genotype. The accumulation of amino acids in tomato genotypes under high alkaline stressed conditions is caused by a shift in the metabolism of carbon and nitrogen components, as well as the concentration effect (Wu et al., 2020; Tareq et al., 2024). A similar increase in glutamate content was observed with salinity stress by Zushi and Matsuzoe (2014) in *Lycopersicon esculentum* Mill. "House Momotaro" (Zushi and Matsuzoe, 2015). An increase in amino acids indicates the stress management strategy of plants treated with ionic (Qiang et al., 2025).

4.4. Effect of alkaline stress on ion homeostasis

Maintaining ion homeostasis and ionic toxicity is a major consequence of alkaline stress in plants, particularly in leaves. Under such conditions, plants often struggle to differentiate between Na^+ and K^+ ions because of their similar physicochemical characteristics. Munns & Tester (2008) (Munns and Tester, 2008) have summarised it into three key tolerance mechanisms used by plants to compare ionic stress, ion exclusion, tissue tolerance, and osmotic tolerance (Kamanga et al., 2023). In this study, the alkaline-sensitive genotype M56 accumulated significantly higher amounts of Na^+ in the shoots (Fig. 6A), while maintaining stable K^+ levels (Fig. 6B), in contrast to the alkaline-tolerant genotype A10. Gene expression analysis showed that the tomato *HKT1;1, HKT1;2*, and *SOS1* genes, which encode Na^+ selective class I-HKT transporters, were differentially expressed. Specifically, *HKT1;2* was expressed in both the leaves and roots of the A10 genotype. The high expression of *HKT1;2* in alkaline condition root tissue suggests enhanced removal of Na^+ from the xylem into the xylem parenchymal cells, thereby reducing its transport to young leaves. Similar findings were reported by Almeida et al. (2017) (Almeida et al., 2017) and Ali et al. (2018) (Ali et al., 2018) (Fig. 2C and F). In contrast, *HKT1;1* was expressed in both the leaves and roots of M56, while its expression was very low expression in A10 (Fig. 2B and E). Interestingly, the expression of *HKT1;1* was correlated with higher Na^+ accumulation. This is unexpected, as the tomato *HKT1;2* sequence is more like *AtHKT1;1* than to tomato *HKT1;1* (Davenport et al., 2007), and *AtHKT1;1* expression in roots is associated with reduced Na^+ accumulation in shoots (Ali et al., 2018; Jaime-Pérez et al., 2017; Romero-Aranda et al., 2021). Furthermore, increased alkalinity also results in significant differences in *SOS1* gene expression, part of the SOS signalling pathway for Na^+ extrusion (Wang et al., 2020c; Rao et al., 2021), was significantly upregulated in the leaves of the tolerant genotype A10 under increasing alkalinity (pH 8.2 and 9.2), while its expression was downregulated in the roots of both genotypes. This tissue-specific response suggests differential regulation of Na^+ efflux under stress. Our results demonstrated that genotype A10 maintained higher K^+/Na^+, Ca^{2+}/Na^+, and Mg^{2+}/Na^+ ratios under increasing alkaline stress compared to the sensitive M56 genotype. This trend aligns with established models of salinity and alkalinity tolerance, where ion homeostasis is a key determinant of stress resilience (Van Zelm et al., 2020; Almeida et al., 2017). Previous studies have shown that maintaining a high K^+/Na^+ (Fig. 6 C) ratio is critical for enzyme activity, osmotic adjustment, and overall growth under stress conditions (Van Zelm et al., 2020; Rao et al., 2021). Similarly, a higher Ca^{2+}/Na^+ ratio contributes to membrane stability and mitigates Na^+ toxicity (Hernández-Salinas et al., 2022), while an elevated Mg^{2+}/Na^+ ratio helps sustain chlorophyll content and photosynthetic efficiency (Rao et al., 2023; Xu et al., 2022). Together, these findings confirm that A10's superior ion regulation mechanisms play a central role in its enhanced alkaline stress tolerance and further support the potential use of ion ratios as physiological markers for screening tolerant tomato genotypes. While this study provides comprehensive insights into leaf ionomic adjustments under

alkaline stress, we acknowledge that root ionomics data could further elucidate the role of transporters like *SOS1* and *SlHKT1;1/2* in ion homeostasis (Jaime-Pérez et al., 2017; Wang et al., 2020c). Future studies should integrate root ion profiling to fully resolve genotype-specific uptake and exclusion mechanisms.

The ATI results reinforce the pivotal role of osmolyte accumulation and ion balance in conferring alkaline stress resilience. Traits such as proline, GABA, and total FAAs with ATI values consistently greater than 1 in A10 underline its superior capacity for osmotic adjustment and ROS detoxification under controlled conditions, in line with the well-established function of compatible solutes in stress adaptation (Meena et al., 2019; Mishra et al., 2023). Conversely, ATI values below 1 for M56 at higher pH indicate its limited physiological plasticity, supporting its sensitive response. The observed decline in K^+/Na^+ ATI at increasing pH levels highlights the persistent challenge of maintaining ion homeostasis under alkaline conditions (Van Zelm et al., 2020; Munns and Tester, 2008; Almeida et al., 2017). These patterns align with previous applications of stress tolerance indices (STIs) in salinity research (Rao et al., 2023; Bigot et al., 2023), suggesting that ATI could be a practical screening tool for identifying genotypes with robust physiological mechanisms to withstand alkaline stress.

5. Conclusion

This study provides the first integrated multi-omics analysis of alkaline stress responses in contrasting tomato genotypes, unravelling genotype-specific mechanisms of tolerance through coordinated transcriptomic, biochemical, and ionomic adaptations, which fills critical gaps in understanding genotype-specific alkaline stress responses. We demonstrated that genotype A10 exhibits markedly greater tolerance than M56, attributed to its efficient Na^+ exclusion, superior ion homeostasis, and higher accumulation of osmoprotectants such as proline and polyphenols. The enhanced detoxification capacity through free amino acid metabolism and the coordinated upregulation of key stress-responsive pathways, including MAPK, ethylene, and glutamate decarboxylase (GAD) signalling further strengthen A10's adaptive advantage. Collectively, these insights position A10 as a promising genotype for cultivation in alkaline soils and as a valuable genetic resource for breeding stress-tolerant tomato cultivars. Future studies should explore the interactions between MAPK-ethylene crosstalk and ion transporter regulation, their effects on yield and fruit quality under field conditions, and the potential epigenetic mechanisms governing stress-responsive gene expression to accelerate the development of resilient tomato varieties for sustainable agriculture.

CRediT authorship contribution statement

Bhargava Krishna Ganasula: Writing – original draft, Investigation, Formal analysis, Data curation. Claudia Chiodi: Data analysis & validation. Silvia Celletti: Biochemical analysis, Writing – review & editing. Riccardo Fedeli: FAAs analysis. Saptarathi Deb: Data analysis & editing. Giovanni Bertoldo: Methodology, Investigation. Maria Cristina Della Lucia: Methodology, Investigation. Massimo Cagnin: Ionomic analysis. Luisella Roberta Celi: Methodology, Writing – review & editing. Piergiorgio Stevanato: Writing – review & editing, Conceptualization, Supervision, Project administration, Funding acquisition.

Funding

This study was conducted within the Agritech National Research Center and funded by the European Union's Next-Generation EU program (National Recovery and Resilience Plan [PNRR] Mission 4, Component 2, Investment 1.4-D.D. 1032, June 17, 2022, CN00000022). It serves as a position paper for Spoke 1, "Plant and animal genetic resources and adaptation to climate changes." It establishes a baseline for achieving the milestones outlined in Task 1.2.4: "Profiling plant-microbial associations and enhancing these interactions through biostimulant treatments to improve plant resilience to environmental stressors." This manuscript reflects solely the authors' views and opinions, neither the European Union nor the European Commission bears responsibility for its content.

Declaration of competing interest

The authors declare that they have no known competing financial interests or personal relationships that could have appeared to influence the work reported in this paper.

Appendix A. Supplementary data

Supplementary data to this article can be found online at https://doi.org/10.1016/j.plaphy.2025.110494.

Data availability

The RNA-seq data have been deposited in the ENA database, with SRA accession ID: PRJEB83642 (ERP167232); All data is available from the author upon reasonable request.

References

Abdelmoneim, M.S., Dawood, M.F.A., Hafez, E.E., Hammad, S.F., Ghazy, M.A., 2025. Unveiling the role of cadaverine in mitigating salinity and/or Bisphenol A toxicity in tomato plants and reduced Bisphenol A accumulation in tomato roots. Plant Physiol. Biochem. 224, 109799. https://doi.org/10.1016/j.plaphy.2025.109799.

Al-Duais, M., Müller, L., Böhm, V., Jetschke, G., 2009. Antioxidant capacity and total phenolics of Cyphostemma digitatum before and after processing: use of different assays. Eur. Food Res. Technol. 228, 813–821. https://doi.org/10.1007/s00217-008-0994-8.

Ali, A., Khan, I.U., Jan, M., Khan, H.A., Hussain, S., Nisar, M., et al., 2018. The high-affinity potassium transporter EpHKT1;2 from the *extremophile Eutrema parvula* mediates salt tolerance. Front. Plant Sci. 9. https://doi.org/10.3389/fpls.2018.01108.

Ali, A.A.M., Romdhane, W.B., Tarroum, M., Al-Dakhil, M., Al-Doss, A., Alsadon, A.A., et al., 2021. Analysis of salinity tolerance in Tomato introgression lines based on morpho-physiological and molecular traits. Plants 10, 2594. https://doi.org/10.3390/plants10122594.

Almeida, D.M., Oliveira, M.M., Saibo, N.J.M., 2017. Regulation of Na^+ and K^+ homeostasis in plants: towards improved salt stress tolerance in crop plants. Genet. Mol. Biol. 40, 326–345. https://doi.org/10.1590/1678-4685-gmb-2016-0106.

Arnon, D.I., 1950. Prof. D. R. Hoagland. Nature 165, 56–58. https://doi.org/10.1038/165056a0.

Assouguem, A., Joutei, A.B., Lahlali, R., Kara, M., Bari, A., Ali, E.A., et al., 2024. Evaluation of the impact of two citrus plants on the variation of *Panonychus citri* (Acari: tetranychidae) and beneficial phytoseiid mites. Open Life Sci. 19. https://doi.org/10.1515/biol-2022-0837.

Aung, T.T., Shi, F., Zhai, Y., Xue, J., Wang, S., Ren, X., et al., 2022. Acidic and alkaline conditions affect the growth of tree peony plants via altering photosynthetic characteristics, limiting nutrient assimilation, and impairing ROS balance. IJMS 23, 5094. https://doi.org/10.3390/ijms23095094.

Babraham Bioinformatics - FastQC A quality control tool for high throughput sequence Data n.d. https://www.bioinformatics.babraham.ac.uk/projects/fastqc/. (Accessed 17 July 2025).

Bates, L.S., Waldren, R.P., Teare, I.D., 1973. Rapid determination of free proline for water-stress studies. Plant Soil 39, 205–207. https://doi.org/10.1007/bf00018060.

Bigot, S., Fuksová, M., Martínez, J.-P., Lutts, S., Quinet, M., 2023. Sodium and chloride accumulation and repartition differed between the cultivated tomato (*Solanum lycopersicum*) and its wild halophyte relative *Solanum chilense* under salt stress. Sci. Hortic. 321, 112324. https://doi.org/10.1016/j.scienta.2023.112324.

Chapman, J.M., Muhlemann, J.K., Gayomba, S.R., Muday, G.K., 2019. RBOH-Dependent ROS synthesis and ROS scavenging by plant specialized metabolites to modulate plant development and stress responses. Chem. Res. Toxicol. 32, 370–396. https://doi.org/10.1021/acs.chemrestox.9b00028.

Chen, R.-D., Yu, L.-X., Greer, A.F., Cheriti, H., Tabaeizadeh, Z., 1994. Isolation of an osmotic stress- and abscisic acid-induced gene encoding an acidic endochitinase from *Lycopersicon chilense*. Mol. Gen. Genet. 245, 195–202. https://doi.org/10.1007/bf00283267.

Chen, N., Qin, J., Tong, S., Wang, W., Jiang, Y., 2022. One AP2/ERF transcription factor positively regulates Pi Uptake and drought tolerance in poplar. IJMS 23, 5241. https://doi.org/10.3390/ijms23095241.

Cheng, M.-C., Liao, P.-M., Kuo, W.-W., Lin, T.-P., 2013. The Arabidopsis ETHYLENE RESPONSE FACTOR1 regulates abiotic stress-responsive gene expression by binding to different cis-acting elements in response to different stress signals. Plant Physiol. 162, 1566–1582. https://doi.org/10.1104/pp.113.221911.

Cohen, S.A., Michaud, D.P., 1993. Synthesis of a fluorescent derivatizing reagent, 6-Aminoquinolyl-N-Hydroxysuccinimidyl carbamate, and its application for the analysis of hydrolysate amino acids via high-performance liquid chromatography. Anal. Biochem. 211, 279–287. https://doi.org/10.1006/abio.1993.1270.

Davenport, R.J., Muñoz-Mayor, A., Jha, D., Essah, P.A., Rus, A., Tester, M., 2007. The na $^{+}$ transporter AtHKT1;1 controls retrieval of Na^{+} from the xylem in *Arabidopsis*. Plant Cell Environ. 30, 497–507. https://doi.org/10.1111/j.1365-3040.2007.01637.x.

Fang, S., Hou, X., Liang, X., 2021. Response mechanisms of plants under saline-alkali stress. Front. Plant Sci. 12. https://doi.org/10.3389/fpls.2021.667458.

FAO, 2024. Pag- 150. doi: 10.4060/cd3044en.

Fedeli, R., Vannini, A., Celletti, S., Maresca, V., Munzi, S., Cruz, C., et al., 2023. Foliar application of wood distillate boosts plant yield and nutritional parameters of chickpea. Ann. Appl. Biol. 182, 57–64. https://doi.org/10.1111/aab.12794.

Fischer, R., Maurer, R., 1978. Drought resistance in spring wheat cultivars. I. Grain yield responses. Aust. J. Agric. Res. 29, 897. https://doi.org/10.1071/ar9780897.

Ge, S.X., Son, E.W., Yao, R., 2018. iDEP: an integrated web application for differential expression and pathway analysis of RNA-Seq data. BMC Bioinf. 19. https://doi.org/10.1186/s12859-018-2486-6.

Gharbi, E., Martínez, J.-P., Benahmed, H., Lepoint, G., Vanpee, B., Quinet, M., et al., 2017. Inhibition of ethylene synthesis reduces salt-tolerance in tomato wild relative species *Solanum chilense*. J. Plant Physiol. 210, 24–37. https://doi.org/10.1016/j.jplph.2016.12.001.

Ghorbani, M., Azarnejad, N., Carril, P., Celletti, S., Loppi, S., 2024. Boosting the resilience to drought of crop plants using wood distillate: a pilot study with lettuce (*Lactuca sativa* L.). Plant Stress 12, 100450. https://doi.org/10.1016/j.stress.2024.100450.

Goodstein, D.M., Shu, S., Howson, R., Neupane, R., Hayes, R.D., Fazo, J., et al., 2012. Phytozome: a comparative platform for green plant genomics. Nucleic Acids Res. 40, D1178–D1186. https://doi.org/10.1093/nar/gkr944.

Guo, M., Wang, X.-S., Guo, H.-D., Bai, S.-Y., Khan, A., Wang, X.-M., et al., 2022. Tomato salt tolerance mechanisms and their potential applications for fighting salinity: a review. Front. Plant Sci. 13. https://doi.org/10.3389/fpls.2022.949541.

Gzik, A., 1996. Accumulation of proline and pattern of α-amino acids in sugar beet plants in response to osmotic, water and salt stress. Environ. Exp. Bot. 36, 29–38. https://doi.org/10.1016/0098-8472(95)00046-1.

Hernández-Salinas, M., Valdez-Aguilar, L.A., Alia-Tejacal, I., Alvarado-Camarillo, D., Cartmill, A.D., 2022. Silicon enhances the tolerance to moderate NaCl-salinity in tomato grown in a hydroponic recirculating system. J. Plant Nutr. 45, 413–425. https://doi.org/10.1080/01904167.2021.1963772.

Hosmani, P.S., Flores-Gonzalez, M., Van De Geest, H., Maumus, F., Bakker, L.V., Schijlen, E., et al., 2019. An improved de novo assembly and annotation of the tomato reference genome using single-molecule sequencing, Hi-C proximity ligation and optical maps. https://doi.org/10.1101/767764.

Hu, S., Zhao, R., Yang, J., Wang, Z., Hu, X., 2024. Spermidine mediated endogenous nitric oxide coordinately boosts stability through antioxidant capacity and Na+/K+ transporters in tomato under saline-alkaline stress. Sci. Hortic. 329, 112973. https://doi.org/10.1016/j.scienta.2024.112973.

Igamberdiev, A.U., Kleczkowski, L.A., 2018. The glycerate and phosphorylated pathways of serine synthesis in plants: the branches of plant glycolysis linking carbon and nitrogen metabolism. Front. Plant Sci. 9. https://doi.org/10.3389/fpls.2018.00318.

Jaime-Pérez, N., Pineda, B., García-Sogo, B., Atares, A., Athman, A., Byrt, C.S., et al., 2017. The sodium transporter encoded by the HKT1;2 gene modulates sodium/potassium homeostasis in tomato shoots under salinity. Plant Cell Environ. 40, 658–671. https://doi.org/10.1111/pce.12883.

Jang, H.J., Song, M.W., Lee, N.-K., Paik, H.-D., 2018. Antioxidant effects of live and heat-killed probiotic Lactobacillus plantarum Ln1 isolated from kimchi. J. Food Sci. Technol. 55, 3174–3180. https://doi.org/10.1007/s13197-018-3245-4.

Ji, W., Cong, R., Li, S., Li, R., Qin, Z., Li, Y., et al., 2016. Comparative proteomic analysis of soybean leaves and roots by iTRAQ provides insights into response mechanisms to short-term salt stress. Front. Plant Sci. 7. https://doi.org/10.3389/fpls.2016.00573.

Kamanga, R.M., Kopa, F., Kamala, F.D., Sefasi, A., Ndakidemi, P.A., 2023. Screening and evaluation of salinity stress tolerance in local malawian tomato Cultivars. Plant Physiol Rep 28, 259–271. https://doi.org/10.1007/s40502-023-00718-8.

Karakan, F.Y., Kaymak, H.C., Akan, S., Ercisli, S., Assouguem, A., Ullah, R., et al., 2024. Revealing the effects of amino acid, organic acid, and phytohormones on the germination of tomato seeds under salinity stress. Open Life Sci. 19. https://doi.org/10.1515/biol-2022-0892.

Kaspal, M., Kanapaddalagamage, M.H., Ramesh, S.A., 2021. Emerging roles of γ *aminobutyric acid* (GABA) gated channels in plant stress tolerance. Plants 10, 2178. https://doi.org/10.3390/plants10102178.

Khan, S., Sehar, Z., Nidhi, Albaqami M., Khan, N.A., 2023. Ethylene crosstalk with isoprenoid-derived signaling molecules in the context of salinity tolerance. Environ. Exp. Bot. 212, 105379. https://doi.org/10.1016/j.envexpbot.2023.105379.

Langmead, B., Salzberg, S.L., 2012. Fast gapped-read alignment with Bowtie 2. Nat. Methods 9, 357–359. https://doi.org/10.1038/nmeth.1923.

Li, H., Handsaker, B., Wysoker, A., Fennell, T., Ruan, J., Homer, N., et al., 2009. The Sequence Alignment/Map format and SAMtools. Bioinformatics 25, 2078–2079. https://doi.org/10.1093/bioinformatics/btp352.

Li, W., Zhao, F., Fang, W., Xie, D., Hou, J., Yang, X., et al., 2015. Identification of early salt stress responsive proteins in seedling roots of upland cotton (*Gossypium hirsutum* L.) employing iTRAQ-based proteomic technique. Front. Plant Sci. 6. https://doi.org/10.3389/fpls.2015.00732.

Liu, C., Li, J., Zhu, P., Yu, J., Hou, J., Wang, C., et al., 2019. Mulberry EIL3 confers salt and drought tolerances and modulates ethylene biosynthetic gene expression. PeerJ 7, e6391. https://doi.org/10.7717/peerj.6391.

Liu, X., Yu, Y., Liu, Q., Deng, S., Jin, X., Yin, Y., et al., 2020. A Na2CO3-Responsive chitinase gene from Leymus chinensis improve pathogen resistance and saline-alkali stress tolerance in transgenic tobacco and maize. Front. Plant Sci. 11. https://doi.org/10.3389/fpls.2020.00504.

Meena, M., Divyanshu, K., Kumar, S., Swapnil, P., Zehra, A., Shukla, V., et al., 2019. Regulation of L-proline biosynthesis, signal transduction, transport, accumulation and its vital role in plants during variable environmental conditions. Heliyon 5, e02952. https://doi.org/10.1016/j.heliyon.2019.e02952.

Mishra, V., Gahlowt, P., Singh, S., Dubey, N.K., Singh, S.P., Tripathi, D.K., et al., 2023. GABA: a key player of abiotic stress regulation. Plant Signal. Behav. 18. https://doi.org/10.1080/15592324.2022.2163343.

Munns, R., Tester, M., 2008. Mechanisms of salinity tolerance. Annu. Rev. Plant Biol. 59, 651–681. https://doi.org/10.1146/annurev.arplant.59.032607.092911.

Neina, D., 2019. The role of soil pH in plant nutrition and soil remediation. Appl. Environ. Soil Sci. 2019, 1–9. https://doi.org/10.1155/2019/5794869.

Pan, Y., Seymour, G.B., Lu, C., Hu, Z., Chen, X., Chen, G., 2012. An ethylene response factor (ERF5) promoting adaptation to drought and salt tolerance in tomato. Plant Cell Rep. 31, 349–360. https://doi.org/10.1007/s00299-011-1170-3.

Peng, J., Li, Z., Wen, X., Li, W., Shi, H., Yang, L., et al., 2014. Salt-Induced stabilization of EIN3/EIL1 confers salinity tolerance by deterring ROS accumulation in arabidopsis. PLoS Genet. 10, e1004664. https://doi.org/10.1371/journal.pgen.1004664.

Pi, E., Zhu, C., Fan, W., Huang, Y., Qu, L., Li, Y., et al., 2018. Quantitative phosphoproteomic and metabolomic analyses reveal GmMYB173 optimizes flavonoid metabolism in soybean under salt stress. Mol. Cell. Proteomics 17, 1209–1224. https://doi.org/10.1074/mcp.ra117.000417.

Qiang, Q., Zhang, Z., Li, X., Li, C., Mao, M., Ding, X., et al., 2025. The amino acid permease SlAAP6 contributes to tomato growth and salt tolerance by mediating branched-chain amino acid transport. Horticulture Research 12, uhae286. https://doi.org/10.1093/hr/uhae286.

Quagliata, G., Abdirad, S., Celletti, S., Sestili, F., Astolfi, S., 2023. Screening of *Triticum turgidum* genotypes for tolerance to drought stress. Plant Physiol. Biochem. 194, 271–280. https://doi.org/10.1016/j.plaphy.2022.11.025.

Ramos-Ruiz, R., Martinez, F., Knauf-Beiter, G., 2019. The effects of GABA in plants. Cogent Food Agric. 5, 1670553. https://doi.org/10.1080/23311932.2019.1670553.

Rao, Y.R., Ansari, M.W., Sahoo, R.K., Wattal, R.K., Tuteja, N., Kumar, V.R., 2021. Salicylic acid modulates ACS, NHX1, sos1 and HKT1;2 expression to regulate ethylene overproduction and Na^{+}ions toxicity that leads to improved physiological status and enhanced salinity stress tolerance in tomato plants cv. Pusa Ruby. Plant Signaling & Behavior 16. https://doi.org/10.1080/15592324.2021.1950888.

Rao, Y., Peng, T., Xue, S., 2023. Mechanisms of plant saline-alkaline tolerance. J. Plant Physiol. 281, 153916. https://doi.org/10.1016/j.jplph.2023.153916.

Raudvere, U., Kolberg, L., Kuzmin, I., Arak, T., Adler, P., Peterson, H., et al., 2019. g: Profiler: a web server for functional enrichment analysis and conversions of gene lists (2019 update). Nucleic Acids Res. 47, W191–W198. https://doi.org/10.1093/nar/gkz369.

Raziq, A., Wang, Y., Mohi Ud Din, A., Sun, J., Shu, S., Guo, S., 2022. A comprehensive evaluation of salt tolerance in Tomato (Var. Ailsa Craig): responses of physiological and transcriptional changes in rboh's and ABA biosynthesis and signalling genes. IJMS 23, 1603. https://doi.org/10.3390/ijms23031603.

Romero-Aranda, M.R., Espinosa, J., González-Fernández, P., Jaime-Fernández, E., Traverso, J.Á., Asins, M.J., et al., 2021. Role of Na+ transporters HKT1;1 and HKT1;2 in tomato salt tolerance. I. Function loss of *cheesmaniae* alleles in roots and aerial parts. Plant Physiol. Biochem. 168, 282–293. https://doi.org/10.1016/j.plaphy.2021.10.018.

Rong, W., Qi, L., Wang, A., Ye, X., Du, L., Liang, H., et al., 2014. The ERF transcription factor TaERF3 promotes tolerance to salt and drought stresses in wheat. Plant Biotechnol. J. 12, 468–479. https://doi.org/10.1111/pbi.12153.

Sanna, M., Gilardi, G., Gullino, M.L., Mezzalama, M., 2022. Evaluation of physical and chemical disinfection methods of Brassica oleracea seeds naturally contaminated with *Xanthomonas campestris* pv. *campestris*. J. Plant Dis. Prot. 129, 1145–1152. https://doi.org/10.1007/s41348-022-00635-2.

Schmittgen, T.D., Livak, K.J., 2008. Analyzing real-time PCR data by the comparative CT method. Nat. Protoc. 3, 1101–1108. https://doi.org/10.1038/nprot.2008.73.

Shah, W.H., Rasool, A., Saleem, S., Mushtaq, N.U., Tahir, I., Hakeem, K.R., et al., 2021. Understanding the integrated pathways and mechanisms of transporters, protein kinases, and transcription factors in plants under salt stress. International Journal of Genomics 2021, 1–16. https://doi.org/10.1155/2021/5578727.

Shang, C., Liu, X., Chen, G., Zheng, H., Khan, A., Li, G., et al., 2024. *SlWRKY80*-mediated jasmonic acid pathway positively regulates tomato resistance to saline–alkali stress by enhancing spermidine content and stabilizing Na^{+}/K^{+} homeostasis. Horticulture Research 11. https://doi.org/10.1093/hr/uhae028.

Sharma, A., Shahzad, B., Rehman, A., Bhardwaj, R., Landi, M., Zheng, B., 2019. Response of phenylpropanoid pathway and the role of polyphenols in plants under abiotic stress. Molecules 24, 2452. https://doi.org/10.3390/molecules24132452.

Shelp, B.J., Aghdam, M.S., Flaherty, E.J., 2021. γ-*Aminobutyrate* (GABA) regulated plant defense: mechanisms and opportunities. Plants 10, 1939. https://doi.org/10.3390/plants10091939.

Shi, Y., Zhang, Z., Yan, Z., Chu, H., Luo, C., 2025. Tomato mitogen-activated protein kinase: mechanisms of adaptation in response to biotic and abiotic stresses. Front. Plant Sci. 16. https://doi.org/10.3389/fpls.2025.1533248.

Tareq, F.S., Singh, J., Ferreira, J.F.S., Sandhu, D., Suarez, D.L., Luthria, D.L., 2024. A targeted and an untargeted metabolomics approach to Study the phytochemicals of tomato cultivars grown under different salinity conditions. J. Agric. Food Chem. 72, 7694–7706. https://doi.org/10.1021/acs.jafc.3c08498.

Thakare, A.P., Della Lucia, M.C., Mulagala, C., Bertoldo, G., Cagnin, M., Stevanato, P., 2024. Omics based approaches to decipher the leaf ionome and transcriptome

changes in *Solanum lycopersicum* L. upon Tomato brown Rugose fruit virus (ToBRFV) infection. PLoS One 19, e0313335. https://doi.org/10.1371/journal.pone.0313335.
The state of food security and nutrition in the world 2021. FAO, IFAD, UNICEF, WFP and WHO. https://doi.org/10.4060/cb4474en, 2021.
Tsai, H.-H., Schmidt, W., 2021. The enigma of environmental pH sensing in plants. Nat. Plants 7, 106–115. https://doi.org/10.1038/s41477-020-00831-8.
Van Zelm, E., Zhang, Y., Testerink, C., 2020. Salt tolerance mechanisms of plants. Annu. Rev. Plant Biol. 71, 403–433. https://doi.org/10.1146/annurev-arplant-050718-100005.
Wang, N., Zhao, J., He, X., Sun, H., Zhang, G., Wu, F., 2015. Comparative proteomic analysis of drought tolerance in the two contrasting Tibetan wild genotypes and cultivated genotype. BMC Genom. 16. https://doi.org/10.1186/s12864-015-1657-3.
Wang, J., Zhang, Y., Yan, X., Guo, J., 2020a. Physiological and transcriptomic analyses of yellow horn (*Xanthoceras sorbifolia*) provide important insights into salt and saline-alkali stress tolerance. PLoS One 15, e0244365. https://doi.org/10.1371/journal.pone.0244365.
Wang, W.-R., Liang, J.-H., Wang, G.-F., Sun, M.-X., Peng, F.-T., Xiao, Y.-S., 2020b. Overexpression of PpSnRK1α in tomato enhanced salt tolerance by regulating ABA signaling pathway and reactive oxygen metabolism. BMC Plant Biol. 20. https://doi.org/10.1186/s12870-020-02342-2.
Wang, Z., Hong, Y., Li, Y., Shi, H., Yao, J., Liu, X., et al., 2020c. Natural variations in SlSOS1 contribute to the loss of salt tolerance during tomato domestication. Plant Biotechnol. J. 19, 20–22. https://doi.org/10.1111/pbi.13443.
Wang, Y., Shen, B., Yang, L., Wang, D., 2022. Integrated analysis of the transcriptome and metabolome in young and mature leaves of *Yunnanopilia longistaminea*. Plant Biotechnol Rep 16, 553–564. https://doi.org/10.1007/s11816-022-00771-z.
Wang, H., Ye, L., Zhou, L., Yu, J., Pang, B., Zuo, D., et al., 2023. Co-Expression network analysis of the transcriptome identified hub genes and pathways responding to saline–alkaline stress in Sorghum bicolor L. IJMS 24, 16831. https://doi.org/10.3390/ijms242316831.
Wang, J., Zhang, Y., Wang, J., Ma, F., Wang, L., Zhan, X., et al., 2024. Promoting *γ-aminobutyric acid* accumulation to enhances saline-alkali tolerance in tomato. Plant Physiol. 196, 2089–2104. https://doi.org/10.1093/plphys/kiae446.
Wei, H., Wang, X., Zhang, Z., Yang, L., Zhang, Q., Li, Y., et al., 2024. Uncovering key salt-tolerant regulators through a combined eQTL and GWAS analysis using the super pan-genome in rice. Natl. Sci. Rev. 11. https://doi.org/10.1093/nsr/nwae043.
Wu, X., Jia, Q., Ji, S., Gong, B., Li, J., Lü, G., et al., 2020. Gamma-aminobutyric acid (GABA) alleviates salt damage in tomato by modulating Na+ uptake, the GAD gene, amino acid synthesis and reactive oxygen species metabolism. BMC Plant Biol. 20, 465. https://doi.org/10.1186/s12870-020-02669-w.
Wu, Q., Su, N., Huang, X., Cui, J., Shabala, L., Zhou, M., et al., 2021. Hypoxia-induced increase in GABA content is essential for restoration of membrane potential and preventing ROS-induced disturbance to ion homeostasis. Plant Communications 2, 100188. https://doi.org/10.1016/j.xplc.2021.100188.
Xu, Z., Wang, J., Zhen, W., Sun, T., Hu, X., 2022. Abscisic acid alleviates harmful effect of saline–alkaline stress on tomato seedlings. Plant Physiol. Biochem. 175, 58–67. https://doi.org/10.1016/j.plaphy.2022.01.018.
Yan, S., Gao, Y., Tian, M., Tian, Y., Li, J., 2021. Comprehensive evaluation of effects of various carbon-rich amendments on tomato production under continuous saline water irrigation: overall soil quality, plant nutrient uptake, crop yields and fruit quality. Agric. Water Manag. 255, 106995. https://doi.org/10.1016/j.agwat.2021.106995.
Yang, Y., Wang, L., Tian, J., Li, J., Sun, J., He, L., et al., 2012. Proteomic study participating the enhancement of growth and salt tolerance of bottle gourd rootstock-grafted watermelon seedlings. Plant Physiol. Biochem. 58, 54–65. https://doi.org/10.1016/j.plaphy.2012.05.026.
Yang, S., Xu, Y., Tang, Z., Jin, S., Yang, S., 2024. The impact of alkaline stress on plant growth and its alkaline resistance mechanisms. IJMS 25, 13719. https://doi.org/10.3390/ijms252413719.
Ye, J., Coulouris, G., Zaretskaya, I., Cutcutache, I., Rozen, S., Madden, T.L., 2012. Primer-BLAST: a tool to design target-specific primers for polymerase chain reaction. BMC Bioinf. 13. https://doi.org/10.1186/1471-2105-13-134.
Yu, H., Wang, T., 2016. Proteomic dissection of endosperm Starch granule associated proteins reveals a network coordinating starch biosynthesis and amino acid metabolism and glycolysis in rice endosperms. Front. Plant Sci. 7. https://doi.org/10.3389/fpls.2016.00707.
Yu, Y., Kim, H.S., Ma, P., Jia, Z., Guo, X., Xie, Y., et al., 2020. A novel ethylene-responsive factor IbERF4 from sweetpotato negatively regulates abiotic stress. Plant Biotechnol Rep 14, 397–406. https://doi.org/10.1007/s11816-020-00612-x.
Zhang, G., Chen, M., Li, L., Xu, Z., Chen, X., Guo, J., et al., 2009. Overexpression of the soybean GmERF3 gene, an AP2/ERF type transcription factor for increased tolerances to salt, drought, and diseases in transgenic tobacco. J. Exp. Bot. 60, 3781–3796. https://doi.org/10.1093/jxb/erp214.
Zhang, L., Li, Z., Quan, R., Li, G., Wang, R., Huang, R., 2011. An AP2 domain-containing gene, *ESE1*, targeted by the ethylene signaling component EIN3 is important for the salt response in *Arabidopsis*. Plant Physiol. 157, 854–865. https://doi.org/10.1104/pp.111.179028.
Zhang, M., Han, F., Chen, H., Yao, J., Li, Q., Li, Z., et al., 2022a. The effect of salinity on ammonium-assimilating biosystems in hypersaline wastewater treatment. Sci. Total Environ. 829, 154622. https://doi.org/10.1016/j.scitotenv.2022.154622.
Zhang, X., Du, H., Shi, Q., Gong, B., 2022b. Loss of GSNOR increases abiotic stress sensitivity via regulating MAPK-ethylene cascade signaling in *Solanum lycopersicum* L. Environ. Exp. Bot. 199, 104872. https://doi.org/10.1016/j.envexpbot.2022.104872.
Zhang, M., Liu, Z., Fan, Y., Liu, C., Wang, H., Li, Y., et al., 2022c. Characterization of GABA-Transaminase gene from mulberry (*Morus multicaulis*) and its role in salt stress tolerance. Genes 13, 501. https://doi.org/10.3390/genes13030501.
Zhang, L., Sun, Y., Ji, J., Zhao, W., Guo, W., Li, J., et al., 2023. Flavonol synthase gene MsFLS13 regulates saline-alkali stress tolerance in alfalfa. The Crop Journal 11, 1218–1229. https://doi.org/10.1016/j.cj.2023.05.003.
Zushi, K., Matsuzoe, N., 2015. Metabolic profile of organoleptic and health-promoting qualities in two tomato cultivars subjected to salt stress and their interactions using correlation network analysis. Sci. Hortic. 184, 8–17. https://doi.org/10.1016/j.scienta.2014.12.030.